Ferroelectric properties of epitaxial $Pb(Zr,Ti)O_3$ thin films on silicon by control of crystal orientation

Matthijn Dekkers, Minh D. Nguyen, Ruud Steenwelle, Paul M. te Riele, Dave H. A. Blank, and Guus Rijnders[a)]
MESA+ Institute for Nanotechnology, Faculty of Science and Technology, University of Twente, P.O. Box 217, 7500AE Enschede, The Netherlands

(Received 3 April 2009; accepted 31 May 2009; published online 7 July 2009)

Crystalline $Pb(Zr,Ti)O_3$ (PZT) thin films between metallic-oxide $SrRuO_3$ (SRO) electrodes were prepared using pulsed laser deposition on CeO_2/yttria-stabilized zirconia buffered silicon (001) substrates. Different deposition conditions for the initial layers of the bottom SRO electrode result in an orientation switch. Either (110)- or (001)-oriented SRO thin films are obtained and the PZT films deposited on the bottom electrode continued both growth directions. The ferroelectric characteristics of the SRO/PZT/SRO capacitors are found to be strongly dependent on their crystalline orientation: PZT (001)-oriented thin films showed stable, high quality ferroelectric response, while the remnant polarization of the PZT (110)-oriented thin films only show high response after multiple switching cycles. © *2009 American Institute of Physics*.
[DOI: 10.1063/1.3163057]

Ferroelectric oxides, such as $Pb(Zr,Ti)O_3$ (PZT), are useful for electronic and photonic devices, as well as piezomechanical actuators and sensors. The ferro and piezoelectric properties are strongly related to the crystal orientation of the PZT layer. Integration of these devices into silicon technology is therefore not only dependent on the possibility of epitaxial growth on silicon substrates using appropriate buffer layers, but also on the control of the crystallographic orientation. Furthermore, for long-term operation of devices, consistent switching over many cycles of the applied electric field is required. The tendency for the remnant polarization of the ferroelectric capacitors to decrease after repeated switching cycles (fatigue) forms a major problem.[1–3] This indicates that a stable ferroelectric response of the PZT is not straightforward and the response should be better controlled and understood.

It is well known that the performance of a ferroelectric capacitor is strongly influenced by the electrode material since it affects the fatigue behavior, leakage current, dielectric properties, as well as the growth and crystalline structure of ferroelectric films.[3–5] To overcome the problem of fatigue, conducting-oxide electrodes such as RuO_2,[6] $SrRuO_3$ (SRO),[7] $LaNiO_3$,[8] and $(La,Sr)CoO_3$ (Ref. 9) have been used in PZT devices. Although it is recognized that all-oxide devices can diminish fatigue, several other mechanisms affect the stability of the ferroelectric response as well.[10] Especially the influence of the structure and orientation of PZT thin films is usually studied separately from the type of buffer layers, since different buffer layers or electrode materials are required to switch the crystal orientation of epitaxial PZT films on silicon.

In this work, PZT films with different out-of-plane crystal orientations are deposited on silicon substrates by pulsed laser deposition (PLD) without changing the buffer layers. A deposition procedure has been developed to control the crystalline properties of the SRO electrodes and PZT capacitors. This enables the growth of ferroelectric devices with equivalent buffer layers and thicknesses on silicon substrates, but with different crystallographic orientations of the PZT. The ferroelectric properties can therefore be directly related to the crystallographic structure of PZT.

The 250-nm-thick PZT (Zr/Ti 52/48) films are sandwiched between 100 nm SRO electrodes. This stack is deposited on CeO_2 (50 nm)/yttria-stabilized zirconia (YSZ) (50 nm) buffered silicon (001) substrates. All layers are subsequently grown without breaking the vacuum by PLD using a KrF excimer laser (248 nm). More experimental details are described elsewhere.[11] Only the deposition conditions during the growth of the first 4 Å of the SRO bottom electrode are changed in order to obtain (001)-instead of (110)-oriented PZT films. Crystalline properties and epitaxial relationship were investigated by x-ray diffraction (XRD) using a Bruker D8 Discover. The $200 \times 200\ \mu m^2$ capacitors are patterned by lithography process and structured by argon etching of the top electrode and wet etching (HF–HCl solution) of PZT. Polarization-electric field (*P*-*E*) hysteresis loops were measured using a modified Sawyer–Tower circuit (AixACCT TF Analyzer 2000). During these measurements, the films were subjected to bipolar triangular switching cycles at a frequency of 1 kHz and with 200 kV/cm amplitude.

YSZ grows epitaxially on silicon, and can scavenge the native oxide on the surface of the substrate.[12] This allows reproducible coherent growth on non HF-dipped Si substrates. CeO_2 is often used as a second buffer layer to overcome the large mismatch between YSZ and perovskites such as SRO. The in-plane mismatch between the fluorite CeO_2 and pseudocubic SRO is only 2.2% if the perovskite cube is rotated 45°. Since the perovskite PZT almost matches SRO, its crystallographic growth orientation consequently continues that of the underlying electrode.

Figure 1(a) shows the θ-2θ XRD profiles of the PZT/SRO films on CeO_2/YSZ/Si when SRO is grown under normal conditions (600 °C, 0.1 mbar). The epitaxial relationship between the buffer layers and silicon is $CeO_2(001) \| YSZ(001) \| Si(001)$, as expected. However, the

a)Electronic mail: a.j.h.m.rijnders@utwente.nl.

 © 2009 American Institute of Physics

Downloaded 18 Jul 2009 to 130.89.6.57. Redistribution subject to AIP license or copyright; see http://apl.aip.org/apl/copyright.jsp

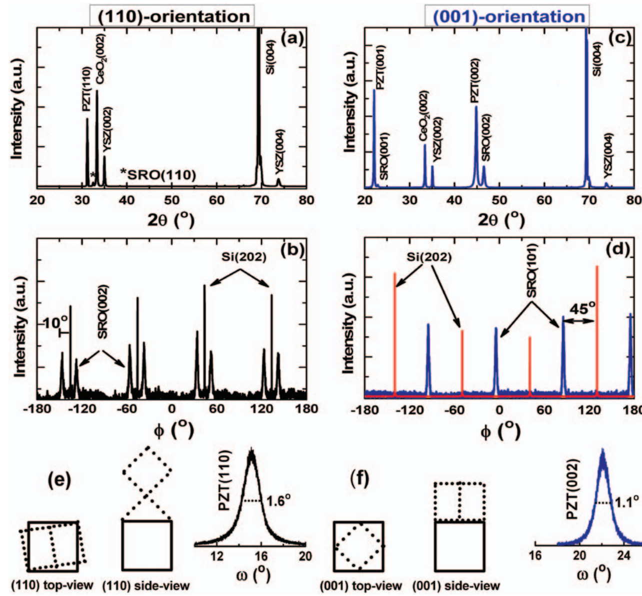

FIG. 1. (Color) XRD patterns of PZT/SRO thin films on $CeO_2(001)/YSZ(001)/Si(001)$, with PZT(110) (a) and PZT(001) (c) orientation respectively. ϕ-scan profiles of SRO(002) and Si(202) reflections of the PZT(110) (b) and PZT(001) sample (d). Schematic side and top view of the SRO(110) (e) and SRO(001) (f) configuration (dashed) on $CeO_2(001)$ (solid) and corresponding ω-scan rocking curves of PZT(110) and PZT(002) peaks.

PZT/SRO layers grow (110)-oriented according to PZT(110)∥SRO(110)∥CeO_2(001)∥YSZ(001)∥Si(001). In-plane analysis of this sample by means of ϕ scans is shown in Fig. 1(b). Four identical sets of peaks of SRO(002) are positioned around the reflections corresponding to Si(202). Since two SRO(002) peaks are expected in a perfect crystal, this means that twin domains exist in the thin film. Furthermore, instead of a single peak positioned at the Si(202) position, the intensity is divided over two peaks situated at +10° and –10° with respect to Si. This in-plane rotation corresponds to an alignment of the SRO⟨111⟩ unit-cell body diagonal with the ⟨110⟩ face diagonal of CeO_2 as illustrated in Fig. 1(e). This in-plane epitaxy has been earlier observed by Hou *et al.*[13] on the single buffer layer of YSZ. These authors assumed that the SRO⟨111⟩∥YSZ/Si⟨110⟩ arrangement was preferred above the 45° rotated cube-on-cube SRO⟨110⟩∥YSZ/Si⟨100⟩ relation because of the smaller mismatch of the former compared to the latter. Since CeO_2 is used as a second buffer layer however, the lattice mismatch is larger in our case. Nevertheless, the SRO⟨111⟩∥YSZ/Si⟨110⟩ in-plane epitaxy is still preferred. We assume that the specific stoichiometric ratio of the elements during the growth of the first SRO monolayers is responsible for this preferred orientation. Sr and Ru are both present on the CeO_2 surface after the first pulses as both materials are ablated in equal amounts from the stoichiometric target. The SRO unit cell consists of a layered $SrO-RuO_2-SrO$ structure. Given that both Sr and Ru exist in the (110) plane in equal amounts, the (110) growth orientation of the perovskite block is promoted if both elements are present. On the other hand, if SrO is used as a starting layer, (001)-oriented growth is expected. Because of the higher volatility of Ru, the stoichiometric ratio of Sr and Ru can be changed drastically if the deposition temperature is increased.[14] Consequently, the first 20 pulses SRO (~4 Å) are deposited at high temperature (800 °C) and reducing O_2 environment (<10^{-5} mbar) allowing Ru evaporation. Evidenced by x-ray photoelectron spectroscopy (not shown), the starting layer is now Sr-rich. As a result, the formed SrO layer acts as a base plane for the perovskite block. Continued growth of SRO at 600 °C results in (001)-oriented growth of the electrode and the PZT layer as is clear from Fig. 1(c). The ϕ scans in Fig. 1(d) shows a 45° shift of the SRO(202) compared to the Si(202) fourfold symmetry related peaks. This proves that the unit cells of SRO/PZT/SRO are rotated on the CeO_2/YSZ/Si stack as schematically drawn in Fig. 1(f).

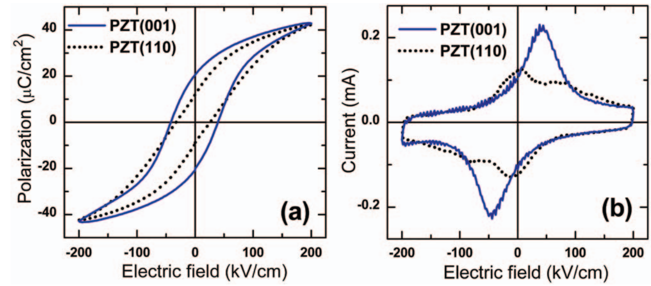

FIG. 2. (Color) *P-E* hysteresis (a) and *I-V* loops (b) of PZT(001) and PZT(110) samples at 1 kHz frequency.

The *P-E* hysteresis loops and *I-V* switching currents of the PZT films with different crystalline orientations are shown in Figs. 2(a) and 2(b), respectively. The PZT(001) film shows a classical ferroelectric polarization loop; whereas the polarization loop of the PZT(110) film is noticeably degraded. The remnant polarization (P_r) in the PZT(110) film is considerably lower compared to the (001)-oriented film (13.5 $\mu C/cm^2$ compared to 20.1 $\mu C/cm^2$, respectively). Whereas the current of the PZT(001)-oriented film shows only one peak when the ferroelectric domains are switched, for the PZT(110)-oriented film, two peaks appear. The peak associated with switching of the ferroelectric domains appears at higher electrical fields than for the PZT (001)-oriented film. The second peak in the switching current at zero voltage is attributed to a nonferroelectric phase which is apparently present in this film.

Subsequently, both films are subjected to a high number of switching cycles in order to monitor the ferroelectric response stability. As illustrated in Fig. 3, the PZT thin film using SRO electrodes in this study show essentially no fatigue; i.e., P_r is not decreasing as the number of switching cycles is increased. For the PZT(001)-oriented film P_r remains constant up to 10^8 cycles. On the other hand, the PZT (110)-oriented film shows an improvement of P_r from 13.5 to 18 $\mu C/cm^2$. P_r now almost equals that of the PZT(001) film. Furthermore, the polarization loop and switching current after 10^8 cycles in Figs. 3(b) and 3(c) look similar for both samples. Figure 4(a) shows switching current transients versus electric field (*I-E*) with various cycle numbers for the PZT(110) film. In the initial stage the switching current peak shows a dramatic broadening and it is separated into two distinct peaks in the *I-E* curve. The current peak amplitude at higher field increases with continuous switching cycling. Simultaneously, the current peak amplitude around zero decreases and eventually disappears. The latter corresponds to a nonferroelectric switching behavior that vanishes after multiple switching cycles. It is known that if samples are

Downloaded 18 Jul 2009 to 130.89.6.57. Redistribution subject to AIP license or copyright; see http://apl.aip.org/apl/copyright.jsp

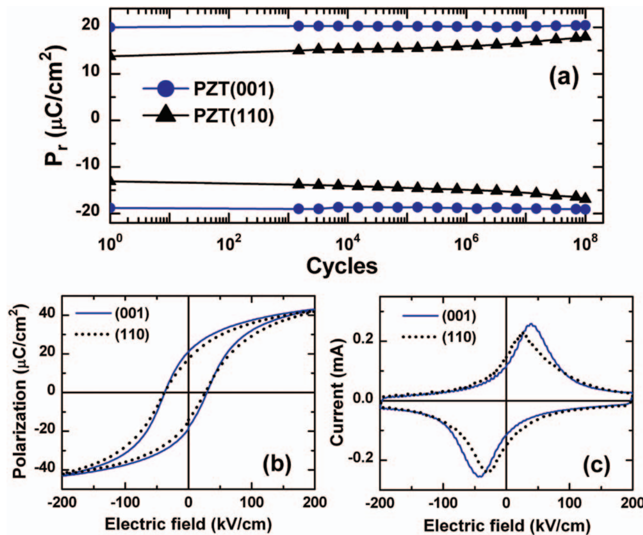

FIG. 3. (Color) Remnant polarization of PZT(001) and PZT(110) samples versus the number of switching cycles at 200 kV/cm amplitude and 1 kHz frequency (a). *P-E* hysteresis (b) and *I-V* loops (c) of PZT(001) and PZT(110) samples after 10^8 cycles.

leaky due to defects such as grain boundaries, this can suppress ferroelectric response. The different dynamic ferroelectric behavior of both films most likely originates from the difference in structural properties. Although grain boundaries do exist in the PZT(001) film, the separated grains are oriented coherently in-plane. This is in contrast with the PZT(110) film, where the in-plane coherence is poor, as is shown by Fig. 1(b). In this case, the structural domains, which are not aligned with respect to each other, exist in the SRO film, hence in the PZT. This also affects the out-of-plane coherence, as can be seen from the differences between the rocking curves [Figs. 1(e) and 1(f)]. The grain boundaries between the twinned structural domains are formed by defective crystal faces. These disturbed in-plane structural defects form pinning centers for charges and ferroelectric domain walls at the grain boundaries, which significantly increase the leakage current. Figure 4(b) shows the leakage current versus electric field for the (001)- and the (110)-oriented film at the initial stage and after multiple cycling. It is seen that the leakage current of the (001)-oriented film is smaller than that of the (110)-oriented film at the initial stage. After 10^8 cycles, however, the leakage current is similar for both films. Upon switching, the leakage along grain boundaries is reduced by removal of pinning centers for charges. This diminishes the number of shorted polar domains, resulting in a larger total ferroelectric contribution.

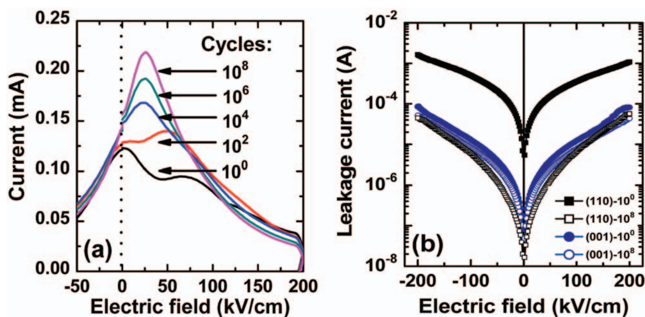

FIG. 4. (Color) Positive part of the *I-V* loop of the PZT(110) sample after 1, 10^2, 10^4, 10^6, and 10^8 switching cycles (a). Leakage current vs electric field characteristics of PZT(001) and PZT(110) samples at initial stage and after 10^8 switching cycles (b).

In conclusion, we have linked the ferroelectric properties to the structure of different crystallographic oriented PZT thin films on silicon substrates. It is shown that, by introducing an extra step in the deposition process, an orientation switch from (110)- to (001)-oriented growth of electrodes and films on similar buffer layers can be realized. The poor in-plane structural coherence of (110) films is responsible for a significant leakage current reducing the ferroelectric response. This is the reason for the unstable ferroelectric behavior of the all-oxide PZT(110) capacitor, as compared to the extremely constant response of the PZT(001) capacitor, showing very low leakage current from the beginning. However, after prolonged switching of the PZT(110) capacitor, the remnant polarization gradually improves because the continued switching slowly removes the leakage paths. Finally, approximately the same properties as for the PZT(001)-capacitor are obtained.

Authors Dekkers and Nguyen both contributed equally to this article. The authors gratefully acknowledge the support of the SmartMix Program of the Netherlands Ministry of Economic Affairs and the Netherlands Ministry of Education, Culture and Science, as well as the Vietnamese Overseas Scholarship Program (Grant No. MOET-VOSP Project 322).

[1] D.-H. Do, P. G. Evans, E. D. Isaacs, D. M. Kim, C. B. Eom, and E. M. Dufresne, Nature Mater. **3**, 365 (2004).
[2] J. F. Scott, *Ferroelectric Memories* (Springer, Berlin, 2000).
[3] A. K. Tagantsev, I. Stolichnov, E. L. Colla, and N. Setter, J. Appl. Phys. **90**, 1387 (2001).
[4] J. J. Lee, C. L. Thio, and S. B. Desu, J. Appl. Phys. **78**, 5073 (1995).
[5] A. Q. Jiang, J. F. Scott, M. Dawber, and C. Wang, J. Appl. Phys. **92**, 6756 (2002).
[6] C. W. Law, K. Y. Tong, J. H. Li, K. Li, and M. C. Poon, Thin Solid Films **354**, 162 (1999).
[7] C. B. Eom, R. B. Van Dover, J. M. Phillips, D. J. Werder, J. H. Marshall, and C. H. Chen, Appl. Phys. Lett. **63**, 2570 (1993).
[8] M.-S. Chen, T.-B. Wu, and J.-M. Wu, Appl. Phys. Lett. **68**, 1430 (1996).
[9] J. Lee, C. H. Choi, B. H. Park, T. W. Noh, and J. K. Lee, Appl. Phys. Lett. **72**, 3380 (1998).
[10] M. Dawber and J. F. Scott, Appl. Phys. Lett. **76**, 1060 (2000).
[11] M. D. Nguyen, K. Karakaya, P. M. te Riele, D. H. A. Blank, and A. J. H. M. Rijnders, Proceedings of the Third IEEE-NEMS, Sanya, China, 6–9 January 2008 (unpublished), p. 315.
[12] S. J. Wang, C. K. Ong, L. P. You, and S. Y. Xu, Semicond. Sci. Technol. **15**, 836 (2000).
[13] S. Y. Hou, J. Kwo, R. K. Watts, J.-Y. Cheng, and D. K. Fork, Appl. Phys. Lett. **67**, 1387 (1995).
[14] G. Rijnders, D. H. A. Blank, J. Choi, and C.-B. Eom, Appl. Phys. Lett. **84**, 505 (2004).

Downloaded 18 Jul 2009 to 130.89.6.57. Redistribution subject to AIP license or copyright; see http://apl.aip.org/apl/copyright.jsp